

High-spin polycarbenes as models for organic ferromagnets

Hiizu Iwamura

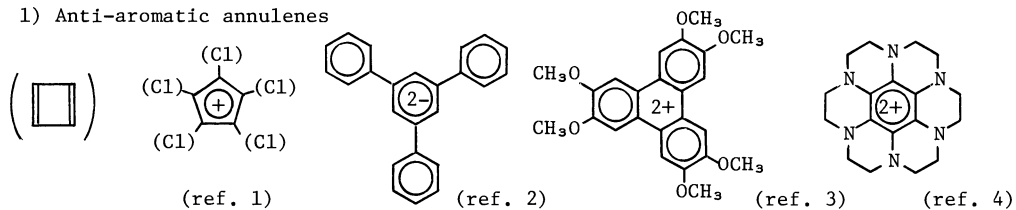
Department of Applied Molecular Science, Institute for Molecular Science,
 Myodaiji, Okazaki 444, Japan

Abstract - In response to the Mataga's prediction of ferromagnetic hydrocarbons (1968), we have taken up the study of two series of high-spin polycarbenes (1 and 2). The corresponding polydiazo compounds were prepared through a series of unambiguous synthetic reactions and photolyzed in 2-methyltetrahydrofuran matrices and in single crystals of a benzophenone host at cryogenic temperatures. The ESR fine structures and magnetic susceptibilities were measured and analyzed to show that the highest spin states were generated as the electronic ground state of 1 and 2. Similarly, isomeric bis(diazo)-[2.2]paracyclophanes were prepared and photolyzed to find, in good agreement with the McConnell's theory on the ferromagnetic intermolecular interaction between organic free radicals (1963), that the pseudoortho and pseudopara dicarbenes have the ground quintet state while the pseudometal isomer is in the ground singlet state. A strategy for increasing the spin ordering over the high-spin aromatic molecules by orienting the stacking mode was thus obtained. Relevance of these results to macroscopic ferromagnets is discussed.

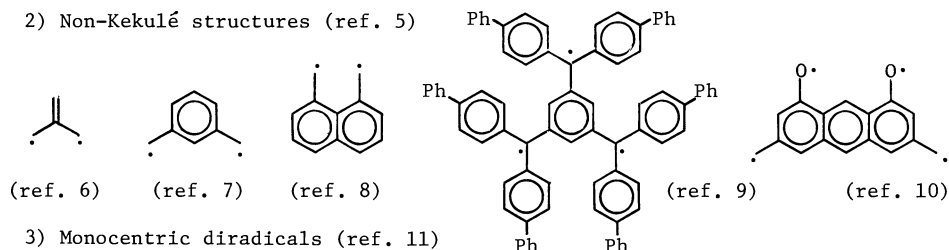
INTRODUCTION

What characterizes organic molecules? Organic molecules are characterized by their closed shell electronic structure. The ground electronic state of organic molecules is singlet and, therefore, most organic compounds are diamagnetic. There are quite a few organic free radicals that have the doublet ground state. These radicals are paramagnetic. Organic molecules known to have the ground triplet and higher spin multiplicity are quite limited. These few compounds are classified into three groups: 1) anti-aromatic annulenes, 2) non-Kekulé structures, and 3) monocentric diradicals. These structures are considered to serve as good starting points for designing organic molecules having even higher spin multiplicity in the ground state. We designed, generated and analyzed a series of high-spin polycarbenes 1 and 2 based on the structural combination of the last two groups. These high-spin hydrocarbons are expected to function as models for hitherto unknown organic ferromagnets.

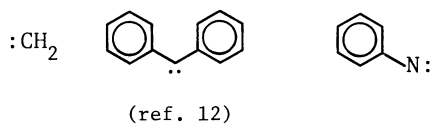
1) Anti-aromatic annulenes



2) Non-Kekulé structures (ref. 5)

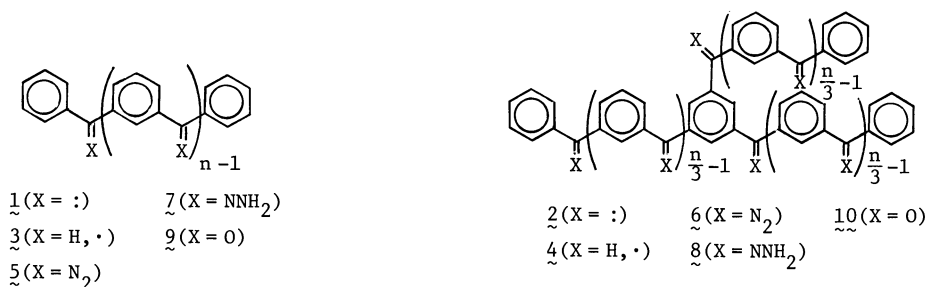


3) Monocentric diradicals (ref. 11)



MOLECULAR DESIGN

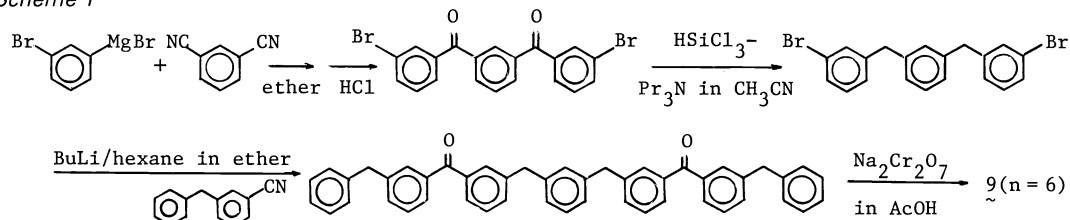
According to the Longuet-Higgins' theory (ref. 13), an alternant hydrocarbon (AH) has at least $N-2T$ singly occupied non-bonding molecular orbitals (NBMO) where N is the number of carbon atoms in the AH and T is the maximum number of double bonds occurring in any resonance structure. Structures **3** and **4** are predicted to have n degenerate NBMO and, therefore, the ground state of the neutral hydrocarbons will be of high spin, i.e., $S = n/2$ by application of Hund's rule. The modern theory by Davidson and Borden (ref. 14) classifies **3** and **4** as non-disjoint, and the ground state is more safely predicted to be of high spin. The recent VB theory also gives the same high-spin multiplicity for these systems (ref. 15). Let us incorporate the monocentric diradical into the above theory. Diphenylcarbene is known to have a ground triplet state (ref. 12). The divalent carbon atom has one NBMO and a nearly degenerate in-plane NBMO localized on the carbon. A large one-center exchange interaction leads to the electronic ground state in which two electrons are incorporated into the two orbitals one each with parallel spin. By replacing each doublet center $>CH\cdot$ in **3** and **4** with the divalent $>C:$, one obtains a series of systems **1** and **2** where $S = n$, doubling the structural efficiency for increasing the total electron spin quantum number. In theory we can put $n \rightarrow \infty$ and predict one-dimensional and two-dimensional macroscopic spins for **1** and **2**, respectively. The $n-\pi$ interaction between the localized n spins and the delocalized π spins in **1** and **2** has a close resemblance to the $s-d$ interaction in ferromagnetic metals, alloys and dilute alloys. The theoretical prediction that these series of compounds would act as ferromagnetic polymers was put forward by Mataga in 1968 (ref. 16) and the lower homologs were reported by Itoh (ref. 17) and Wasserman (ref. 18) in 1967. We have set out on the study of the higher homologs of these series.



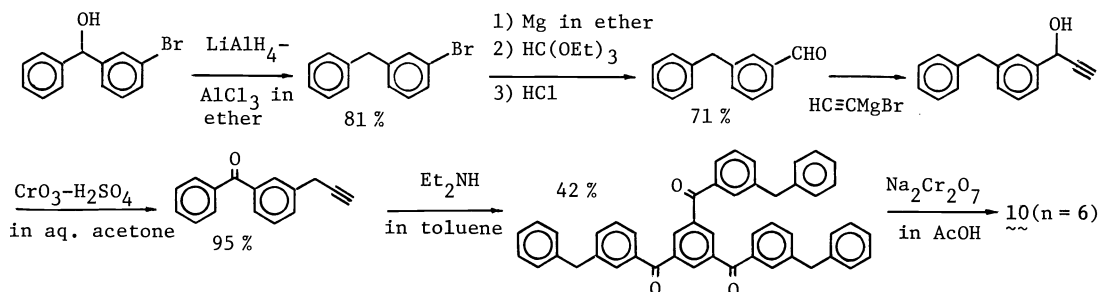
PREPARATION OF THE PRECURSORS

The corresponding polydiazocarbene compounds **5** and **6** are potentially good precursors, since carbenes are cleanly generated by photolysis of diazo compounds. They were obtained by oxidation of the corresponding polyhydrazones **7** and **8** with metal oxides. The polyhydrazones were, in turn, prepared by the reaction of polyketones **9** and **10** with hydrazine. For **9** and **10**, we employed a series of established synthetic reactions as exemplified by the hexamers in Schemes 1 and 2. While the reactions leave no doubt that the structures are correct, we confirmed the latter by means of high-resolution H-1 and C-13 NMR spectroscopy. Polydiazocarbene compounds **5** and **6** gave wine-red microcrystals. The meta disposition of the functional groups leads to interesting spectroscopic properties; $\lambda(\max)$ stays constant at 293 and 519 nm, and molar absorptivity

Scheme 1



Scheme 2



increases in proportion to the number of the units.

PHOTOLYSIS OF THE POLYDIAZO COMPOUNDS AND CHARACTERIZATION OF THE HIGH-SPIN POLYCARBENES

ESR fine structure analysis of the polycarbenes is exemplified by $\underline{1}(n=4)$. The diazo precursor $\underline{5}(n=4)$ was oriented in a single crystal of benzophenone and photolyzed in an ESR cavity at 4.2 K with a 405-nm mercury line. An eight-line spectrum was obtained (Fig. 1) and analyzed in terms of the fine structure due to the following $\Delta M_S = \pm 1$ allowed transitions $A_{\pm}(M_S = \pm 4 \leftrightarrow \pm 3)$, $B_{\pm}(M_S = \pm 3 \leftrightarrow \pm 2)$, $C_{\pm}(M_S = \pm 2 \leftrightarrow \pm 1)$, and $D_{\pm}(M_S = \pm 1 \leftrightarrow \pm 0)$. The relative separations are nearly $(A_- - A_+) : (B_- - B_+) : (C_- - C_+) : (D_- - D_+) = 7 : 5 : 3 : 1$, and the relative integrated intensities are nearly $A_{\pm} : B_{\pm} : C_{\pm} : D_{\pm} = 4 : 7 : 9 : 10$ as expected of $S=4$ in the high-field approximation. The magnetic field is approximately parallel to the Z principal axis of the fine-structure tensor, the deviation being 9.8° , which gives the largest fine-structure splittings.

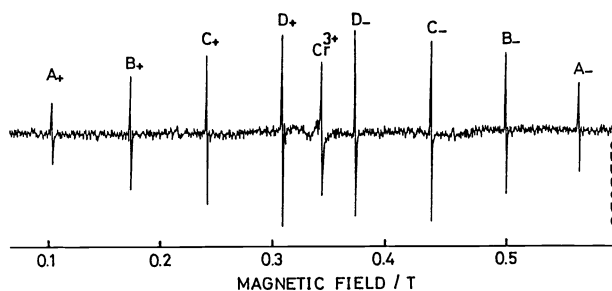


Fig. 1. ESR spectrum of $\underline{1}(n=4)$ obtained at 4.2 K with the magnetic field along the direction 26° from the a axis in the ab plane of the host crystal. The microwave frequency was 9550.6 MHz. The central line is due to Cr^{3+} in MgO powder used as a reference substance (ref. 19).

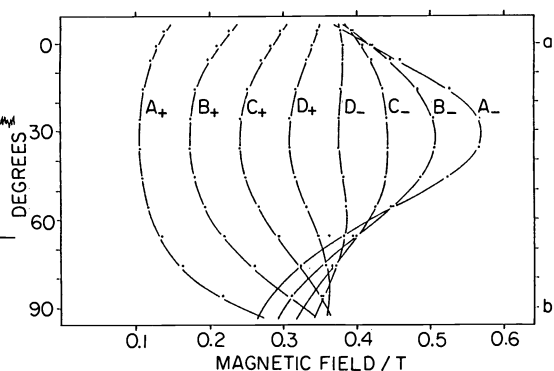


Fig. 2. Angular dependence of the ESR resonance fields of the eight allowed transitions observed at 4.2 K for rotation of the magnetic field (9550.2 MHz) in the ab plane of the benzophenone single crystal containing $\underline{1}(n=4)$ (ref. 20).

The angular dependence of the resonance fields (Fig. 2) and of the signal intensities of the eight lines is well reproduced by the spin Hamiltonian:

$$\mathcal{H} = g\beta\mathbf{H}\cdot\mathbf{S} + D[S_Z^2 - \frac{1}{3}S(S+1)] + E(S_X^2 - S_Y^2) \quad (1)$$

where $S=4$, $g=2.003$, $D=+0.0332 \text{ cm}^{-1}$ and $E=-0.0031 \text{ cm}^{-1}$. Higher terms in S allowed group-theoretically for $S=4$ are negligibly small. This fact and the nearly isotropic g value close to that of the free electron spin are consistent with $\underline{1}(n=4)$ being composed of light atoms with small spin-orbit coupling. In addition, the D and E values fall in the range extrapolated from the known high-spin multiplet hydrocarbons (ref. 21).

In order to determine the lowest energy level, we have measured the ESR spectra in the temperature range 1.8–150 K. No thermally populated triplet, quintet and septet signals were detected, indicating that the ground state is nonet. Plots of the total ESR signal intensity vs reciprocal temperature gave a straight line. If the singlet state were located below the nonet state, a considerable decrease in total intensity should have occurred below 4.2 K.

One sample cut from a single crystal of benzophenone doped with $\underline{1}(n=4)$ showed interesting K-band ESR spectral changes with increasing temperature. After a change at 64 K, the spectrum consisted of a superposition of signals from two magnetically different nonet molecules. These are designated as isomers II and III, while the first nonet molecule observed at 4.2 K after photolysis of $\underline{5}(n=4)$ is isomer I. At 92 K the spectrum showed another transition into isomer IV. All the changes were irreversible. The observed D and E values for the nonet isomers are collected in TABLE 1. Since all the isomers related by the thermal activation are in the nonet ground states and the fine-structure parameters are not very different, the observed spectral changes may most reasonably be interpreted in terms of moderate conformational changes in $\underline{1}(n=4)$. The principal axes of isomers I–IV listed in TABLE 1 provide information on their molecular conformations and orientations in the crystal. The Z axes, which are associated with the long axis of $\underline{1}(n=4)$, are approximately parallel with each other. When the nonet molecule changes its shape as $I \rightarrow II \rightarrow IV$, the Z axis changed its

direction by $\Theta_{I,II}=2^\circ$, $\Theta_{II,IV}=-2^\circ$, while the X and Y axes rotated $\Phi_{I,II}=13^\circ$ and $\Phi_{II,IV}=-12^\circ$ about the old Z axis. On the other hand, the changes I \rightarrow III \rightarrow IV gave $\Theta_{I,III}=6^\circ$ and $\Theta_{III,IV}=-6^\circ$, $\Phi_{I,III}=50^\circ$ and $\Phi_{III,IV}=-48^\circ$. Thus the latter route via the isomer III is accompanied by considerable rotations of the principal axes X and Y. It is noted that the final isomer IV has almost the same fine-structure tensor as that of isomer I both in magnitude and direction; the X, Y and Z axes coincide within 1° .

TABLE 1. The Hamiltonian parameters g, D, E and the fine-structure tensors for the isomers I-IV (ref. 20)

isomer	g	D (cm^{-1})	E (cm^{-1})	principal axes	principal values (cm^{-1})	direction cosines		
						a	b	c
I	2.002	0.03161	-0.00394	X	-0.01448	0.29016	-0.59491	0.74956
				Y	-0.00660	-0.47296	0.59180	0.65276
				Z	0.02107	0.83194	0.54393	0.10965
II (64 K)	2.002	0.03227	-0.00225	X	-0.01301	0.37741	-0.71515	0.58832
				Y	-0.00851	-0.42814	0.42858	0.79562
				Z	0.02151	0.82113	0.55216	0.14443
III (64 K)	2.002	0.03347	-0.00216	X	-0.01332	0.62776	-0.77840	0.00372
				Y	-0.00900	-0.11269	-0.08615	0.98989
				Z	0.02231	0.77021	0.62183	0.14180
IV (92 K)	2.002	0.03241	-0.00403	X	-0.01483	0.29780	-0.60864	0.73544
				Y	-0.00677	-0.46640	0.57943	0.66838
				Z	0.02161	0.83294	0.54206	0.11131

Since the spin-orbit interaction is negligibly small for hydrocarbons $\underline{1}$ and $\underline{2}$, the first order dipole-dipole interaction between the electron spins is regarded as the origin of the fine structure tensor. The ij component of the fine-structure tensor for a high-spin molecule is given by Eq. 2:

$$D_{ij} = (2/3)(3e^2\hbar^2/4m^2c^2)[2!(2S-2)!/(2S)!] \times \sum_{p,q} \langle p(1)q(2) - q(1)p(2) | (r_{12}^{-2}\delta_{ij} - 3i_{12}j_{12})/r_{12}^5 | p(1)q(2) \rangle \quad (2)$$

where $i, j = X, Y$ or Z and $p(k)$ and $q(k)$ are the molecular orbitals occupied by the k -th electron and are orthogonal with each other. We have carried out a semi-empirical calculation of D_{ij} on the assumption that one-center $n-\pi$ interaction is the most important spin-spin interaction. The $n-\pi$ interaction tensor was parameterized from the experimental data on triplet $\underline{1}$ ($n=1$) (ref. 12). Out of 36 possible planar conformations of $\underline{1}$ ($n=4$), A and B gave the calculated values that are in reasonably good agreement with the observed values for isomers I and IV. Whereas conformation A requires replacement of four benzophenone molecules in the host single crystals, it is necessary for form B to replace only three. The latter would fit better in the

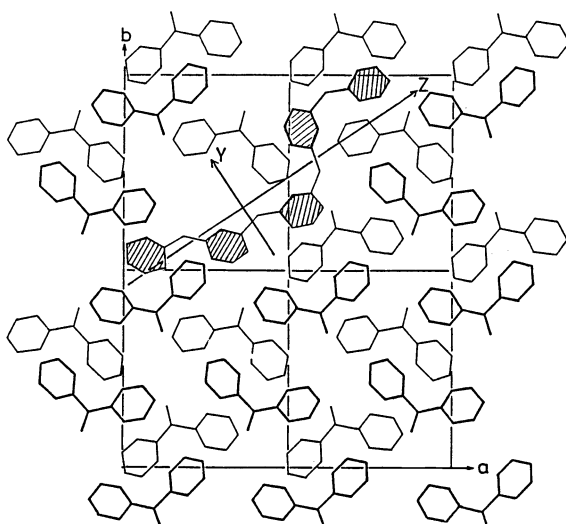
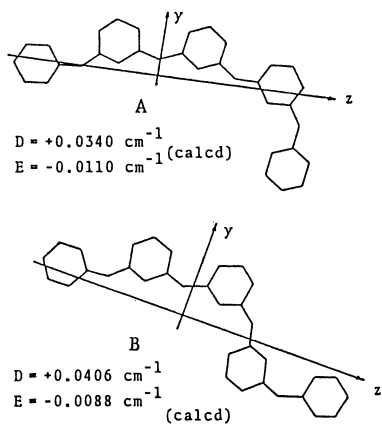


Fig. 3. The orientation of the form B of $\underline{1}$ ($n=4$) in the benzophenone crystal (ref. 20).

host crystals. The projection of form B to the ab plane of the host crystal is shown in Fig. 3. Isomers II and III possess observed fine-structure tensors rather different from those of isomers I and IV (see TABLE 1), both in magnitude and direction. The small E/D values of isomers II and III and the large rotation of the X and Y axes that have accompanied the conformational changes to and from III are not compatible with a planar structure. Rotation of the phenyl rings out of the plane made by C(C:)C has to be taken into account. The important message of this part of the analysis is that $\underline{1}(n=4)$ has the nonet ground state irrespective of its different conformations.

Preliminary results of similar ESR analyses have revealed that $\underline{1}(n=5)$ is in the undecet ($S=5$) and $\underline{1}(n=6)$ and $\underline{2}(n=6)$ are in the tridecet ($S=6$) spin states. These are the highest spin multiplicity ever observed for organic as well as inorganic molecules and ions (ref. 22).

MAGNETIZATION AND MAGNETIC SUSCEPTIBILITY OF HIGH-SPIN POLYCARBENES

Bulk magnetic properties of these organic high-spin species are of paramount interest. We have therefore measured the magnetization of $\underline{1}(n=4)$ as a function of the magnetic field strength and temperature.

Tetracarbene $\underline{1}(n=4)$ doped in crystalline benzophenone

A small cylindrical quartz cell containing crystals of benzophenone doped with $\underline{5}(n=4)$ (5.0×10^{-4} M) was placed in a cryostat of a Faraday-type magnetometer (an Oxford magnetic balance systemized by K. Kimura and S. Bandow of IMS (ref. 23)) and photolyzed by UV irradiation at 4 K to generate $\underline{1}(n=4)$. A main field of 0.5 T was applied by a persistent current mode of the superconducting magnet in order to avoid saturation of magnetization at lower temperatures, the field gradient being kept constant at 0.5 T/m. The diamagnetic susceptibility (χ_d) of the photolyzed sample was determined by the χ vs $1/T$ plot and the value $-0.598 \times 10^{-6} \text{ g}^{-1}$ was subtracted to obtain the paramagnetic susceptibility ($\chi_p = \chi - \chi_d$). The χ_p vs T plots in this system gave a straight line over the whole temperature range (2–100 K) as shown in Fig. 4. The slope of the line, namely the Curie constant, gave $\mu_{\text{eff}} = 9.08 \mu_B$ and therefore the spin number n of 8.1 according to the Curie law:

$$\chi_p = N \mu_{\text{eff}}^2 / 3kT \quad (3)$$

The latter value is in good agreement with the theoretical value of 8. These results clearly show that $\underline{1}(n=4)$ has the nonet spin multiplicity in the ground state and is homogeneously dispersed in the crystal as shown in Fig. 3.

Temperature dependence of χ_p of $\underline{1}(n=4)$ in 2-methyltetrahydrofuran matrix

The magnetic susceptibility of the tetracarbene was then measured in a glassy matrix of 0.2 ml 2-methyltetrahydrofuran (2-MTHF) solution of $\underline{5}(n=4)$ (3.78×10^{-3} M). Plots of $1/\chi_p$ vs T are not represented by a single line (Fig. 5), suggesting that the magnetic interaction between the tetracarbene molecules is now important. The straight line in region A passes through the origin when extrapolated. The individual magnetic moment is considered not to suffer from the

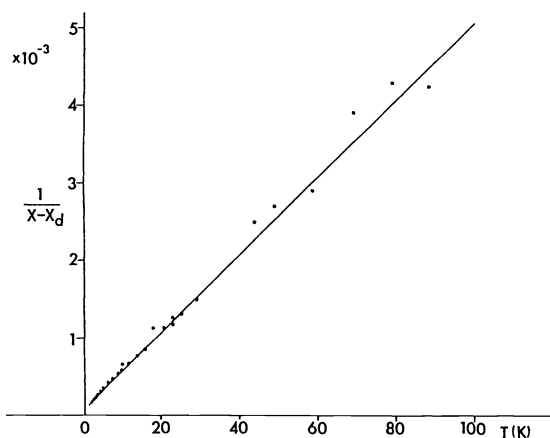


Fig. 4. The temperature dependence of χ_p of $\underline{1}(n=4)$ doped in crystals of benzophenone (5.0×10^{-4} M).

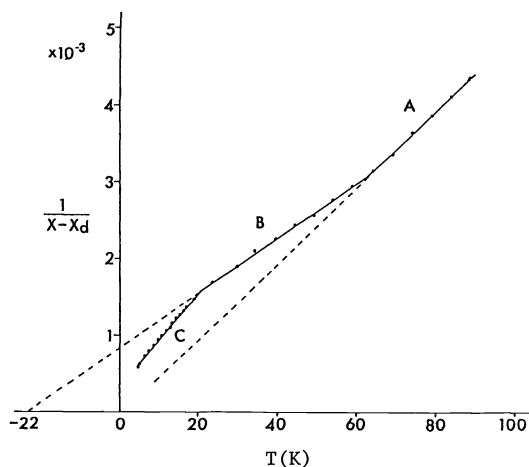


Fig. 5. The temperature dependence of χ_p of $\underline{1}(n=4)$ in a glassy matrix of 2-MTHF (8.7×10^{-4} M) (ref. 24).

molecular field made by the other molecules, presumably because of the thermal fluctuation in their orientation under these conditions. The slope of line A is found to give $\mu_{\text{eff}} = 9.33\mu_B$ and the spin number of 8.4. Deviation of the latter value from 8 is considered to be due to experimental errors. The line has the first break point at 65 K and the line in region B has a negative Weiss temperature $\theta = -22$ K in the Curie-Weiss law:

$$1/\chi_p = 3k(T - \theta)/N\mu_{\text{eff}}^2 \quad (4)$$

indicating that the paramagnetic species now feels the antiferromagnetic molecular field at temperatures below 65 K. After the second break point at ca 20 K, $1/\chi_p$ vs T plots are directed towards the origin (region C). The observed behavior suggests a three-center antiferromagnetic interaction being present among the polycarbene molecules in the matrix as observed in the trinuclear cluster of paramagnetic species (ref. 25). Similar results were obtained when the initial concentration of $\underline{5}(n=4)$ was 3.56×10^{-2} M in 2-MTHF or microcrystals of neat $\underline{5}(n=4)$ were photolyzed. The results show that the polydiaz compound was not evenly dispersed in 2-MTHF matrices, generating carbene molecules close enough to induce antiferromagnetic interaction between them.

Field strength dependence of magnetization of $\underline{1}(n=4)$

Magnetization of $\underline{1}(n=4)$ in 2-MTHF was measured as a function of the main magnetic field at 2.1, 4.2, 9.0, 17.5 and 31 K. The striking feature observed is a large saturation effect of magnetization at lower temperatures. In particular, a complete saturation was observed in the magnetic field higher than 2.5 T at 2.1 K. Such an effect has never been observed for paramagnetic organic compounds. The saturation of magnetization should be due to the high spin multiplicity of $\underline{1}$. When the experimental values are plotted against the field strength over temperature (H/T), the data are found to fit a single curve (Fig. 6). The correlation is rationalized in terms of the Brillouin function for magnetization:

$$B_J(x) = \frac{2J+1}{2J} \coth\left(\frac{2J+1}{2J}x\right) - \frac{1}{2J} \coth\left(\frac{x}{2J}\right) \quad (5)$$

where J is the quantum number of the total angular momentum and $x = gJ\mu_B H/k_B T$. The theoretical magnetization curves are given in Fig. 6 for five high-spin states $J = 2/2, 4/2, 6/2, 8/2$ and $10/2$, the saturated values of each state being normalized to unity. The experimental values are found to fit the theoretical curve with $J = 8/2$ especially in the small H/T region where intermolecular magnetic interaction is not significant. This means that, although magnetic interaction was suggested to be present in the $1/\chi_p$ vs T plots, the magnitude of this interaction was not large enough to give different saturation curves at each temperature range. Since the orbital angular momentum may be neglected for hydrocarbon $\underline{1}$ and therefore $J = S$, the above correlation provides another evidence for the nonet ground state of $\underline{1}(n=4)$. Since Eq. 5 does not contain the concentration of the electron spins, this analysis is proposed as a simple and versatile method for determining the high spin multiplicity of paramagnetic samples of even unknown concentration.

One of the characteristic features of ferromagnetic materials is a strong saturation of magnetization at weak external field. As the spin multiplicity of polycarbenes $\underline{1}$ and $\underline{2}$ becomes higher, the magnetization behavior will more closely resemble that of ferromagnets. Other conspicuous features of ferromagnets are the spontaneous magnetization and hysteresis in magnetization curves. This latter phenomena of ferromagnetic materials is due to the irreversible transfer of magnetic domain walls. Since we are dealing with a discrete system, a better model with which to compare may be metal fine particles. When the particle size of ferromagnetic metal fine particles becomes less than 30 Å in diameter, they are known to have a single domain structure. In these examples the direction of magnetization can be varied

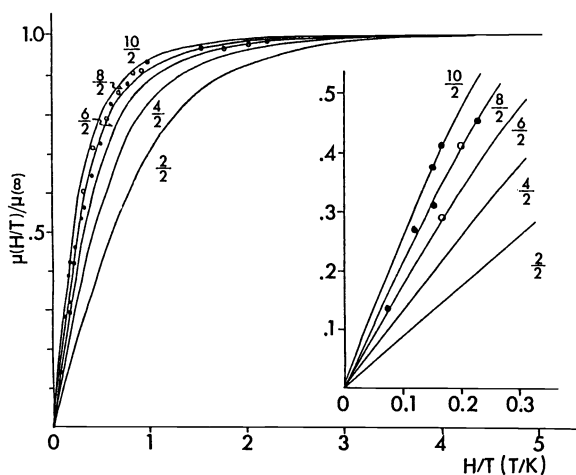


Fig. 6. Plots of magnetization of $\underline{1}(n=4)$ in 2-MTHF vs temperature-normalized field strength (H/T). Theoretical magnetization curves are given by Eq. 5 in which $J = S = 2/2, 4/2, 6/2, 8/2$ and $10/2$, the saturated values being normalized to unity (ref. 24).

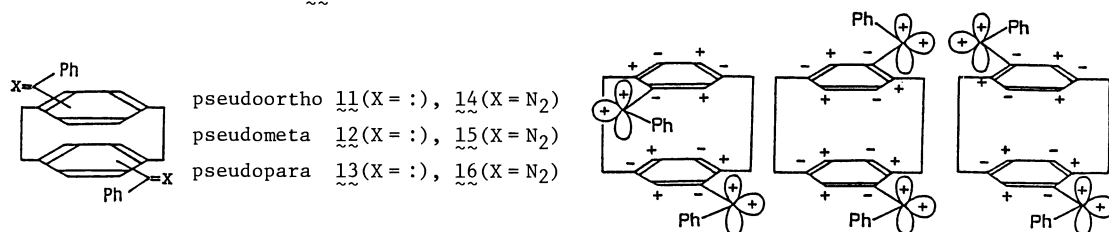
only by rotation of the domain. Thus magnetic anisotropy plays a major role in determining the coercive force. If the anisotropic energy is large enough, the fine particle will show hysteresis and behave as tiny ferromagnets, whereas particles with small anisotropy will be magnetized in any direction without the coercive force. The particles in the latter case are called superparamagnets. The electron spins within a particle can all align in parallel due to the ferromagnetic exchange interaction, but the particles as a whole behave independently of each other as in a paramagnet. Polycarbene $\underline{1}(n=4)$ is best described as the organic molecular superparamagnet.

DESIGN OF FERROMAGNETIC MOLECULAR STACKING OF DIPHENYLCARBENE UNITS

We have been able to demonstrate experimentally that $\underline{1}$ and $\underline{2}$ have high-spin ($S=n$) ground states. We have also found that intermolecular interaction between the randomly formed molecular aggregates of $\underline{1}(n=4)$ in 2-MTHF matrices is antiferromagnetic. In order to develop macroscopic ferromagnetism, it is very important to find a guiding principle under which intermolecular interaction between carbene molecules may become ferromagnetic. There is one such prediction. According to McConnell's theory on intermolecular magnetic interaction (ref. 26), exchange interaction between two aromatic free radicals can be ferromagnetic when the product of spin densities ρ_i and ρ_j at two interacting sites i and j on different molecules A and B is negative in sign, since the exchange integral J_{ij} is negative between organic molecules at a distance of the van der Waals contact (Eq. 6). This theory has never been tested.

$$\mathcal{H}^{AB} = - \sum_{i,j} J_{ij}^{AB} S_i^A \cdot S_j^B = - S^A \cdot S^B \sum_{i,j} J_{ij}^{AB} \rho_i^A \rho_j^B \quad (6)$$

As a model system to test the theory, we took advantage of the [2.2]paracyclophane skeleton. Among the three isomers of bis(phenylmethylene)[2.2]paracyclophanes $\underline{11}$ - $\underline{13}$ with different orientation of the two phenylmethylene substituents, we note that only the pseudoortho and pseudopara isomers satisfy McConnell's condition. From the spin distribution of diphenylcarbene determined by the ENDOR experiments (ref. 12), the sign of the spin density product at each interacting site between the two benzene rings is predicted to be all negative in pseudoortho and pseudopara isomers and all positive in the pseudometa one. Thus the different spin distribution is expected to result in the quintet ground state for $\underline{11}$ and $\underline{13}$ and in the ground singlet state for $\underline{12}$.



Three isomeric dibromo[2.2]paracyclophanes were prepared and separated according to the literature method (ref. 27). Each isomer was dilithiated by *n*-butyllithium in ether and treated with benzaldehyde to give the corresponding diol, which was then oxidized by pyridinium chlorochromate in dichloromethane to give the dibenzoyl[2.2]paracyclophane. This was converted to the didiazo compound through the bis(hydrazone) by oxidizing with yellow HgO in benzene at room temperature. The crude product was purified by alumina column chromatography by rapid elution with benzene: pseudoortho, mp 107-109°C dec; pseudometa, mp 136-138°C dec; pseudopara, mp 147-148°C dec.

Irradiation of $\underline{14}$ in a rigid glass of 2-MTHF at 11 K in an ESR cavity (X-band spectrometer) with Pyrex-filtered UV light gave intense quintet signals as shown in Fig. 7. The zero-field splitting parameters were evaluated to be $|D|=0.0624 \text{ cm}^{-1}$ and $|E|=0.0190 \text{ cm}^{-1}$ on the basis of a third-order perturbational calculation of Eq. 1. The intensity of the quintet signals was found to obey the Curie law in the temperature range 11-50 K, indicating that the quintet is the ground state. A signal at 104.0 mT was detected at temperatures above 20 K. The signal intensity increased at elevated temperatures, suggesting that this species was a thermally populated triplet (T_T), although the rest of its signals were weak and not resolved well (Fig. 8).

In sharp contrast with $\underline{14}$, signals due to the quintet species were not detected in the ESR spectrum obtained after irradiation of $\underline{15}$ (Fig. 9). A new set triplet signals ($T_T: |D|=0.1973 \text{ cm}^{-1}$ and $|E|=0.0038 \text{ cm}^{-1}$) started to appear when the temperature was raised to 20 K. The signal intensities increased as the temperature was raised but did not change with time at each temperature. The signal intensity of T_T started to decrease with time at about 70 K. The intensity behavior is unambiguously of the thermally populated triplet (Fig. 10). Since 1,*n*-biradicals cannot have such large *D* value as observed in T_T , the signals should be due to the triplet state of $\underline{12}$. The absence of quintet signals together with the presence of

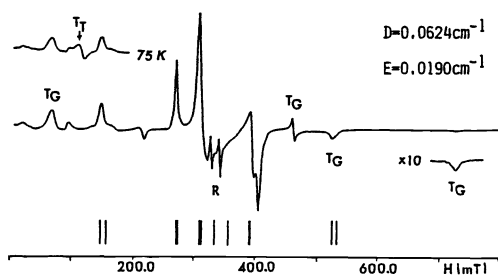


Fig. 7. ESR spectrum obtained after irradiation of $\underline{14}$ in 2-MTHF at 11 K. Lines indicate the calculated transitions of the quintet $\underline{11}$. T_G is assigned to a monocarbene. See text for T_T (ref. 28).

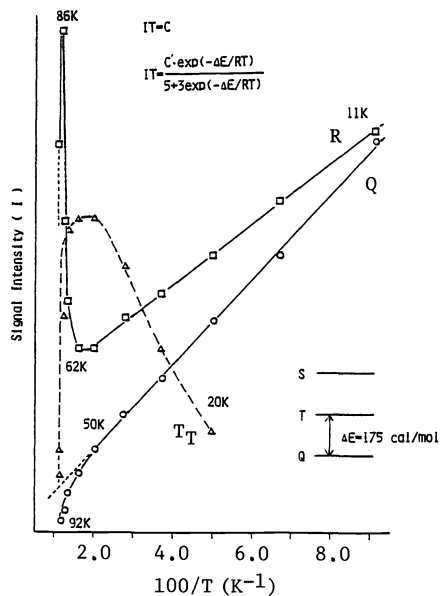


Fig. 8. Plots of the ESR signal intensities vs reciprocal temperatures for the quintet (Q) and triplet (T_T) states of $\underline{11}$.

signals from a thermally populated triplet leads us to conclude that the singlet is the ground state for pseudometa dicarbene $\underline{12}$.

Pseudopara isomer $\underline{16}$ exhibited strong quintet signals due to $\underline{13}$ when photolyzed: $|D| = 0.0718 \text{ cm}^{-1}$ and $E = 0.0041 \text{ cm}^{-1}$. The dicarbene was less stable than the other two isomers and converted thermally at ca 30 K to a biradical ($|D| = 0.0108 \text{ cm}^{-1}$ and $|E| = 0.0005 \text{ cm}^{-1}$). Although the thermal instability of $\underline{13}$ prevented us from drawing the Curie plot over a wide temperature range, the quintet appeared to be the ground state.

The considerable differences in spin multiplicity of dicarbenes $\underline{11}$ - $\underline{13}$ observed above are the first experimental demonstration that the spin distribution of the π -electron in the layered benzenoid moieties can determine the ferro and antiferromagnetic interaction between the free radical species. The results also suggest that the mode of stacking of the benzene units can be crucial in increasing the dimension and determining the intermolecular interaction which should control the bulk magnetic properties of the high-spin aromatic molecules.

CONCLUSION

We have been able to demonstrate that $\underline{1}$ and $\underline{2}$ have the high spin ($S = n$) ground state. The static magnetic susceptibility measurement has revealed that they are strongly paramagnetic. As n increases in $\underline{1}$, the bonding and anti-bonding π -molecular orbitals will become denser and form the valence and conduction bands, respectively (Fig. 11). The NBMO's will form a well-

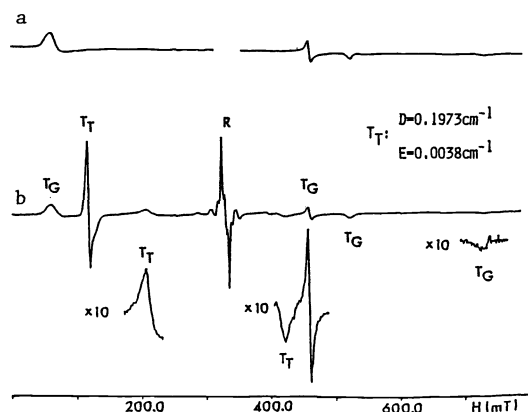


Fig. 9. ESR spectra obtained (a) in the dark after generation of $\underline{12}$ by irradiation of $\underline{15}$ at 11 K, and (b) when (a) was warmed to 60 K. R is due to a biradical formed adventitiously.

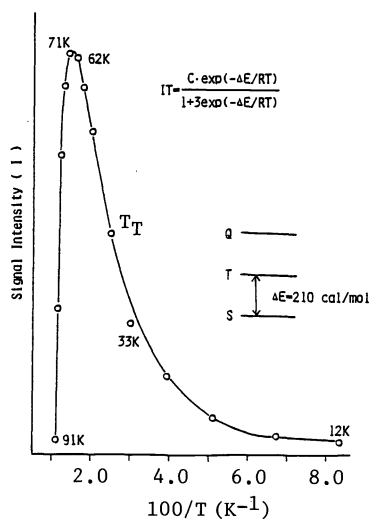


Fig. 10. Plots of the ESR signal intensities vs reciprocal temperatures for the triplet state (T_T) of $\underline{12}$ (ref. 29).

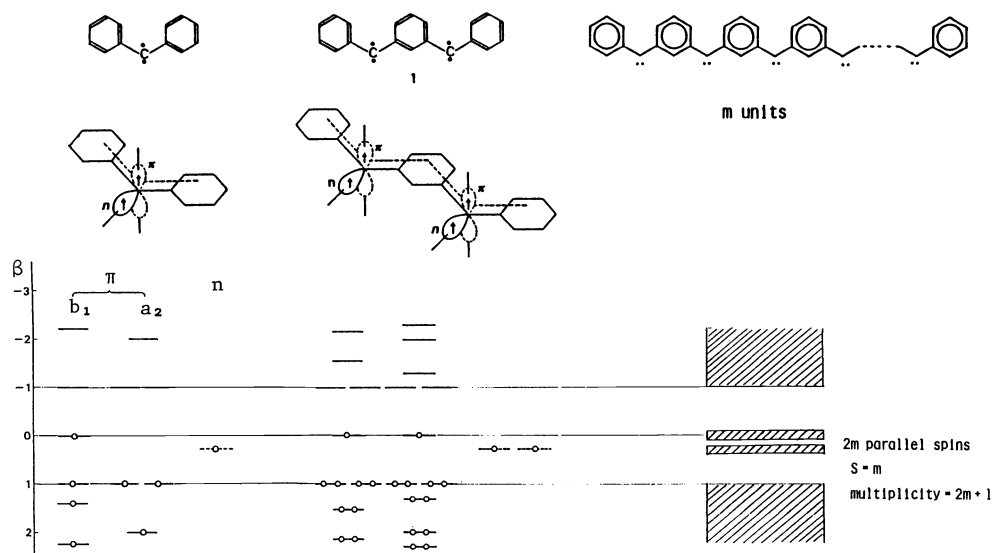


Fig. 11. Molecular orbital characteristics of polycarbenes 1

separated band and, therefore, the spin ordering is considered to remain unperturbed. There is a high chance of obtaining a one-dimensional ferromagnet. Comparison with a typical example of inorganic one-dimensional ferromagnets is worthwhile. In CsNiF_3 and $\text{CoCl}_2 \cdot 2\text{C}_5\text{H}_5\text{N}$ (ref. 30), electron spins on Co atoms, for example, are in a weak ferromagnetic molecular field caused by the exchange interaction within the chain structure. Thus ferromagnetic spin ordering starts to appear at ca 5 K. At lower temperatures, however, antiferromagnetic interchain interaction predominates, resulting in a decrease in magnetic susceptibility. These tendencies are well rationalized by the localized spin model. The ferromagnetic state is realized only in a limited range of cryogenic temperatures. Ferromagnetic metals and dilute alloys are characterized by the presence of conduction spins. Let us consider a linear chain of iron ($3d^6 4s^2$). The ferromagnetic spin ordering of the localized 3d electrons in this hypothetical system would be effected through polarization of the conducting 4s electrons. In the case of polycarbenes 1 and 2, it is the topological symmetry (ref. 31) of AH that gives rise to the degenerate π NBMO's and consequent spin alternation of the π -electrons via strong spin correlation along the molecular chain. The localized n spins are polarized at each carbenic center through a large one center exchange integral $J(\pi|n)$.

The exchange interaction between the molecules of 1 ($n=4$) were found to be antiferromagnetic in the fortuitously formed molecular aggregates in 2-MTHF. However, we were intrigued by the McConnell's theory and have found by model experiments that there are unique stacking modes of the spin-distributed benzene rings of the diphenylcarbene units leading to the high-spin state. Therefore, if we are able to arrange the appropriate molecular stacking of the polycarbenes so that the intermolecular exchange interaction might become ferromagnetic, the high-spin molecules could serve as a magnetic domain and exhibit ferromagnetism as a macroscopic property.

ACKNOWLEDGEMENT

While I am the one who has written this paper, my collaborators cited in the references carried out all of the experiments and analyses. It is only through their talent and hard work that these experiments have succeeded. In particular, I owe the ESR spectral analyses of the oriented polycarbenes to Prof. K. Itoh and his coworkers at Osaka City University. Lastly but not least importantly, I thank Prof. S. Nagakura, Director General of the Institute for his interest and encouragement given to this work.

REFERENCES

1. R. Breslow, R. Hill and E. Wasserman, *J. Am. Chem. Soc.* **86**, 5349-5350 (1964); M. Saunders, R. Berger, A. Jaffe, J. M. McBride, J. O'Neill, R. Breslow, J.M. Hoffman, Jr., C. Perchonock, E. Wasserman, R.S. Hutton and V. J. Kuck, *J. Am. Chem. Soc.* **95**, 3017-3018 (1973).
2. R.E. Jesse, P. Biloen, R. Prins, J.D.W. van Voorst and G.J. Hoijsink, *Mol. Phys.* **6**, 633-635 (1963).
3. R. Breslow, B. Jaun, R.Q. Kluttz and C.Z. Xia, *Tetrahedron*, **38**, 863-867 (1982);

- R. Breslow, Pure Appl. Chem. **54**, 927-938 (1982).
4. R. Reslow, P. Maslak and J.S. Thomaidis, J. Am. Chem. Soc. **106**, 6453-6454 (1984); R. Breslow, Mol. Cryst. Liq. Cryst. **125**, 261-267 (1985).
 5. W.T. Borden, Ed., Diradicals, Wiley, New York (1982).
 6. P. Dowd, J. Am. Chem. Soc. **88**, 2587-2589 (1966); R.J. Crawford and D.M. Cameron, ibid. **88**, 2589-2590 (1966); J.A. Berson, Acc. Chem. Res. **11**, 446-453 (1978).
 7. E. Migirdicyan and J. Baudet, J. Am. Chem. Soc. **97**, 7400-7404 (1975); B.B. Wright and M.S. Platz, ibid. **105**, 628-630 (1983); S. Kato, K. Morokuma, D. Feller, E.R. Davidson and W.T. Borden, ibid. **105**, 1791-1795 (1983).
 8. R. Pagni, M.N. Burnett and J.R. Dodd, J. Am. Chem. Soc. **99**, 1972-1973 (1977).
 9. G. Schmauss, H. Baumgartel and H. Zimmermann, Angew. Chem., Int. Ed. Engl. **4**, 596 (1965); J. Brickmann and G. Kothe, J. Chem. Phys. **59**, 2807-2814 (1973).
 10. D.E. Seeger and J.A. Berson, J. Am. Chem. Soc. **105**, 5144-5146 (1983).
 11. R.A. Moss and M. Jones, Jr., Carbenes II, Chapt. 5 and 6, Wiley, New York (1975).
 12. R.W. Brandon, G.L. Closs and C.A. Hutchison, Jr., J. Chem. Phys. **37**, 1878 (1962); R.W. Murray, A.M. Trozzolo, E. Wasserman and W. A. Yager, J. Am. Chem. Soc. **84**, 3213-3214 (1962); E. Wasserman, L.C. Snyder and W.A. Yager, J. Chem. Phys. **41**, 1763-1772 (1964); R.W. Brandon, G.L. Closs, C.E. Davoust, C.A. Hutchison, Jr., B.E. Kohler and R. Silbey, ibid. **43**, 2006-2016 (1965); C.A. Hutchison, Jr. and B.E. Kohler, ibid. **51**, 3327-3335 (1969).
 13. H.C. Longuet-Higgins, J. Chem. Phys. **18**, 265-274 (1950).
 14. W.T. Borden and E.R. Davidson, J. Am. Chem. Soc. **99**, 4587-4594 (1977).
 15. A.A. Ovchinnikov, Theor. Chim. Acta **47**, 297-304 (1978); D.J. Klein, Pure Appl. Chem. **55**, 299-306 (1983).
 16. N. Mataga, Theor. Chim. Acta **10**, 372-376 (1968).
 17. K. Itoh, Chem. Phys. Lett. **1**, 235-238 (1967).
 18. E. Wasserman, R.W. Murray, W.A. Yager, A.M. Trozzolo and G. Smolinsky, J. Am. Chem. Soc. **89**, 5076-5078 (1967).
 19. Y. Teki, T. Takui, K. Itoh, H. Iwamura and K. Kobayashi, J. Am. Chem. Soc. **105**, 3722-3723 (1983).
 20. Y. Teki, T. Takui, K. Itoh, H. Iwamura and K. Kobayashi, to be published.
 21. T. Takui and K. Itoh, Chem. Phys. Lett. **19**, 120-124 (1973); Y. Teki, T. Takui, H. Yagi, K. Itoh and H. Iwamura, J. Chem. Phys. in press. See also refs. 12, 17 and 18.
 22. W. Weltner, Jr., Magnetic Atoms and Molecules, Van Nostrand Reinhold, New York (1983).
 23. K. Kimura and S. Bandow, Kotai Butsuri (Japanese) **19**, 476-473 (1984).
 24. T. Sugawara, S. Bandow, K. Kimura, H. Iwamura and K. Itoh, J. Am. Chem. Soc. **106**, 6449-6450 (1984).
 25. K. Kambe, J. Phys. Soc. Jpn. **5**, 48-51 (1950); S.J. Gruber, C.M. Harris and E. Sinn, J. Chem. Phys. **49**, 2183-2191 (1968); A.P. Ginsberg, R.L. Martin and R.C. Sherwood, Inorg. Chem. **7**, 932-936 (1968); E. Sinn and C.M. Harris, Coord. Chem. Rev. **4**, 391-422 (1969); E. Sinn, ibid. **5**, 313-347 (1970); T. Idogai, T. Iwashita and N. Uryū, J. Chem. Phys. **54**, 816-817 (1971); I. Morgenstern-Badarau and H.H. Wickman, J. Chem. Soc., Chem. Commun. 176-177 (1985).
 26. H. M. McConnell, J. Chem. Phys. **39**, 1910 (1963).
 27. H.J. Reich and D.J. Cram, J. Am. Chem. Soc. **91**, 3527-3533 (1969).
 28. A. Izuoka, S. Murata, T. Sugawara and H. Iwamura, J. Am. Chem. Soc. **107**, 1786-1787 (1985).
 29. A. Izuoka, S. Murata, T. Sugawara and H. Iwamura, to be published.
 30. B. Steiner, J. Villain and C.G. Windsor, Adv. Phys. **25**, 87-209 (1976); K. Takeda, S. Matsukawa and T. Haseda, J. Phys. Soc. Jpn. **30**, 1330-1336 (1971); Ch. Rosinski and B. Elschner, J. Magnetism Magn. Material **4**, 193-198 (1977).
 31. K. Itoh, Pure Appl. Chem. **50**, 1251-1259 (1978).